

Design, docking study, synthesis and preliminary cytotoxic study of novel Isatin-Niflumic acid derivatives as possible VEGFR tyrosine kinase inhibitors

Hussein Muneam Sahib¹, Ammar Abdulaziz Alibeg²

¹DEPARTMENT OF PHARMACEUTICAL CHEMISTRY, FACULTY OF PHARMACY, UNIVERSITY OF KUFA, NAJAF, IRAQ

²DEPARTMENT OF PHARMACEUTICAL CHEMISTRY, COLLEGE OF PHARMACY, UNIVERSITY OF KUFA, NAJAF, IRAQ

ABSTRACT

Aim: Design, synthesis and cytotoxic evaluation of new series of Isatin-Naiflumic acid derivatives as vascular endothelial growth factor receptor tyrosine kinase inhibitors.

Materials and Methods: A molecular docking study was performed to assess the binding affinities of the synthesized compounds toward the kinase domains of the vascular endothelial growth factor receptor 2. The compounds were synthesized through the esterification process of Niflumic acid, followed by treating the obtained ethyl ester compound with hydrazine monohydrate to form the Niflumic acid hydrazide compound. This compound was further reacted with six Isatin derivatives utilizing the ketone-amine condensation reaction to form the final six Schiff base compounds.

Results: The synthesized compounds (I-VI) showed optimum binding affinity (*S. score*) values ranging from -9.1782 to -9.5120 Kcal/mol and precise binding mode (RMSD) values ranging from 1.0608 to 1.8914 with the active kinase site of the vascular endothelial growth factor receptor 2 (PDB code: 4AG8). At the same time, the cytotoxicity results showed an optimum inhibitory effect (20.87 μ M to 78.48 μ M) against the A549 (non-small cell lung cancer) and a safer effect (175.49 μ M to 280.27 μ M) against the MRC-5 (normal lung tissue cells). In contrast to the reference drug (Sunitinib).

Conclusions: The new synthesized compounds (I-VI) are potent vascular endothelial growth factor receptor 2 tyrosine kinase inhibitors, inhibiting cell proliferation, angiogenesis and exhibiting promising anticancer agents.

KEY WORDS: VEGFR-2 inhibitors, molecular docking, Niflumic acid, Isatin derivatives

Wiad Lek. 2025;78(11):2420-2432. doi: 10.36740/WLek/212543 DOI

INTRODUCTION

Cancer is a lethal illness that remains a major global health concern. It is the second most prevalent illness behind cardiovascular disorders. Consequently, the creation of powerful and efficacious new antineoplastic agents is a primary objective of modern medicinal chemistry [1-2]. A large percentage of clinically licensed anticancer agents have a narrow therapeutic window, mostly because of significant systemic toxicity coupled with pronounced insufficient tumor selectivity [3]. Vascular endothelial growth factor receptors are a principal tumor inducer, as the overexpression of such receptors in malignancies, especially type II triggers an impaired activation of neovascularization signaling pathways that provide adequate oxygen and nutrient demand for accelerated development and proliferation of solid tumors [4-5]. The upregulation of these receptors may serve as a biomarker for the presence of malignant tumors [6]. Consequently, suppressing their pathway would result in efficient anti-angiogenesis and tumor-

igenic response [7]. Despite the availability of several VEGFR inhibitors, clinical resistance and limited efficacy remain major challenges, emphasizing the importance of exploring new scaffolds capable of selectively inhibiting VEGFR-2 tyrosine kinases. Structure-based drug design approach, driven by both literature evidence and the unmet medical need for effective VEGFR-2 inhibitors in cancer therapy. This provided the foundation for docking-guided synthesis and subsequent biological evaluation. Vascular endothelial growth factor receptor 2 (VEGFR-2) is a member of the receptor protein tyrosine kinase (PTK) family that may be categorized into three components: an extracellular ligand binding domain, a transmembrane domain, and a cytoplasmic tyrosine kinase domain [8-9]. At the extracellular part, the vascular endothelial growth factor-A (VEGF-A) binds to VEGFR-2, prompting the development of a homodimer complex of VEGFR-2, modifying the conformation of its intracellular domain. The conformational changes occur induce auto-phosphorylation of the tyrosine residues, leading

to downstream signal transmission and subsequently activating RAS/Raf/MAPK and PI3K/Akt pathways that enhance endothelial cells' proliferation, migration and durability [10]. Inhibitors that compete with adenosine triphosphate (ATP) upon binding to the tyrosine kinases and hindering phosphorylation cascade are considered a crucial chemotherapeutic agent for many types of cancers that show VEGFR-2 overexpression such as in breast cancer renal carcinoma, hepatocellular carcinoma and non-small lung cancer (NSCLC) [11]. In the case of NSCLC, studies show that there is overexpression of VEGFR-2, reaching a value of 54.2% compared to normal tissues [12]. This study involves the design, molecular docking, synthesizing, and toxicity evaluation of compounds derived from the linkage of Isatin. Scaffold with Niflumic acid. Isatin and its derivatives exhibit a wide range of biological actions. The cytotoxic and antineoplastic characteristics have been the most extensively documented among them. The great Isatin scaffold resulted in the production of numerous structurally different derivatives, including analogues derived from many substitutions on the aryl ring, as well as those obtained through derivatization of the Isatin nitrogen and Carbon 2 and 3. These chemicals impede cancer cells multiply and tumor development by interaction with several intracellular targets, including DNA, telomerase, tubulin, P. glycoprotein, protein kinases, and phosphatases [13]. A series of VEGFR-2 inhibitory activity were synthesized and assessed for anticancer potential of Benzofuran-Isatin conjugates against MCF-7, MCF-7/DOX, DU-145, and MDR DU-145 cancer cell lines by MTT assay. The presented results suggested that seven analogues could display better potency with IC_{50} values of 47.6–96.7 μ M against all tested cell lines compared to the positive control sunitinib. SAR results illustrate the carbon spacer between isatin and the benzofuran ring, the isatin motif substituted at C-3 and C-5 positions, and the incorporation of the *para*-substituted phenyl ring at the C-2 position of the benzofuran moiety as required features for significant VEGFR-2 inhibitory and anticancer potential [14]. Niflumic acid is a non-corticosteroid inflammatory suppressor agent often employed in the medical management of rheumatoid arthritis it has lately been recognized as an inhibitor of several malformation cell types, including cancers of the lungs, ovarian, renal, and liver [15].

AIM

The present study aims to design, synthesis and cytotoxic evaluation of new series of Isatin-Niflumic acid derivatives as vascular endothelial growth factor receptor tyrosine kinase inhibitors.

MATERIALS AND METHODS

The reagents as well as solvents used during the synthesis processes were at the laboratory level. Solvents were bought from Central Drug House Ltd., India, and all were dried before being used, while Niflumic acid and Isatin derivatives were bought from Macklin Biochemical Co. Ltd., China. The estimated cost of preparing the proposed Schiff base derivatives is relatively modest when compared to many existing tyrosine kinase inhibitors. The synthetic pathway relies on commercially available starting materials (Isatin and Niflumic acid), which are easily accessible. The conjugation reactions involve acylation and condensation steps that require no costly reagents or specialized equipment, allowing scalability at a reasonable expense. Stuart (SMP30) Melting Point Instrumentation, also was employed to ascertain melting points. Employing one sided open capillary method, the melting points of compounds were determined at the University of Kufa, Faculty of Pharmacy. The melting point describes the point in temperature at which a substance changes from solid to liquid. It's one of the most efficient methods to check compound purity. Thin-layer chromatography in ascending mode was employed to assess how the reaction progressed and determine the degree of its purity, utilizing 0.2 mm silica gel 60F₂₅₄ aluminum plates and a mobile phase composed of hexane and acetone in a proportion (7:3) [16]. Following exposure of silica paper to UV light, a solitary circular spot emerged, demonstrating a complete reaction and a pure yield [17], also, at the University of Kufa Shimadzu (Japan) spectrophotometer, which offers stable Fourier transform infrared spectroscopy analysis (FTIR), was used to obtain compounds spectra. Regarding the magnetic resonance spectra, a Bruker 400 MHz instrument was used to record the ¹H-NMR spectra at the College of Science, University of Basrah. Deuterated solvent (DMSO-d₆) was used to avoid the appearance of misleading or overlapping peaks during the spectra-measuring process [18]. For esterification purposes, Niflumic acid was dissolved in a suitable amount of ethanol, and then the mixture was chilled to before adding an excess amount of thionyl chloride. After that the mixture was refluxed (using a hot plate magnetic stirrer and a glass condenser that was attached to a round-bottomed flask for several hours to obtain the desired Niflumic acid ethyl ester (compound Ia). Then after, the ester aminolysis method is used to convert the obtained ester into amide by reacting (compound Ia) with an excess amount of hydrazine monohydrate 99% in reflux conditions to obtain the desired Niflumic acid hydrazide (compound Ib). Finally, the condensation reaction is utilized by reacting the amine-containing compound (compound Ib) with different types of ketones (Isatin derivatives) under slightly acidic conditions to obtain the final six acyl hydrazone compounds (Schiff bases). The overall synthesis procedure is shown in Figure 1 [19-20].

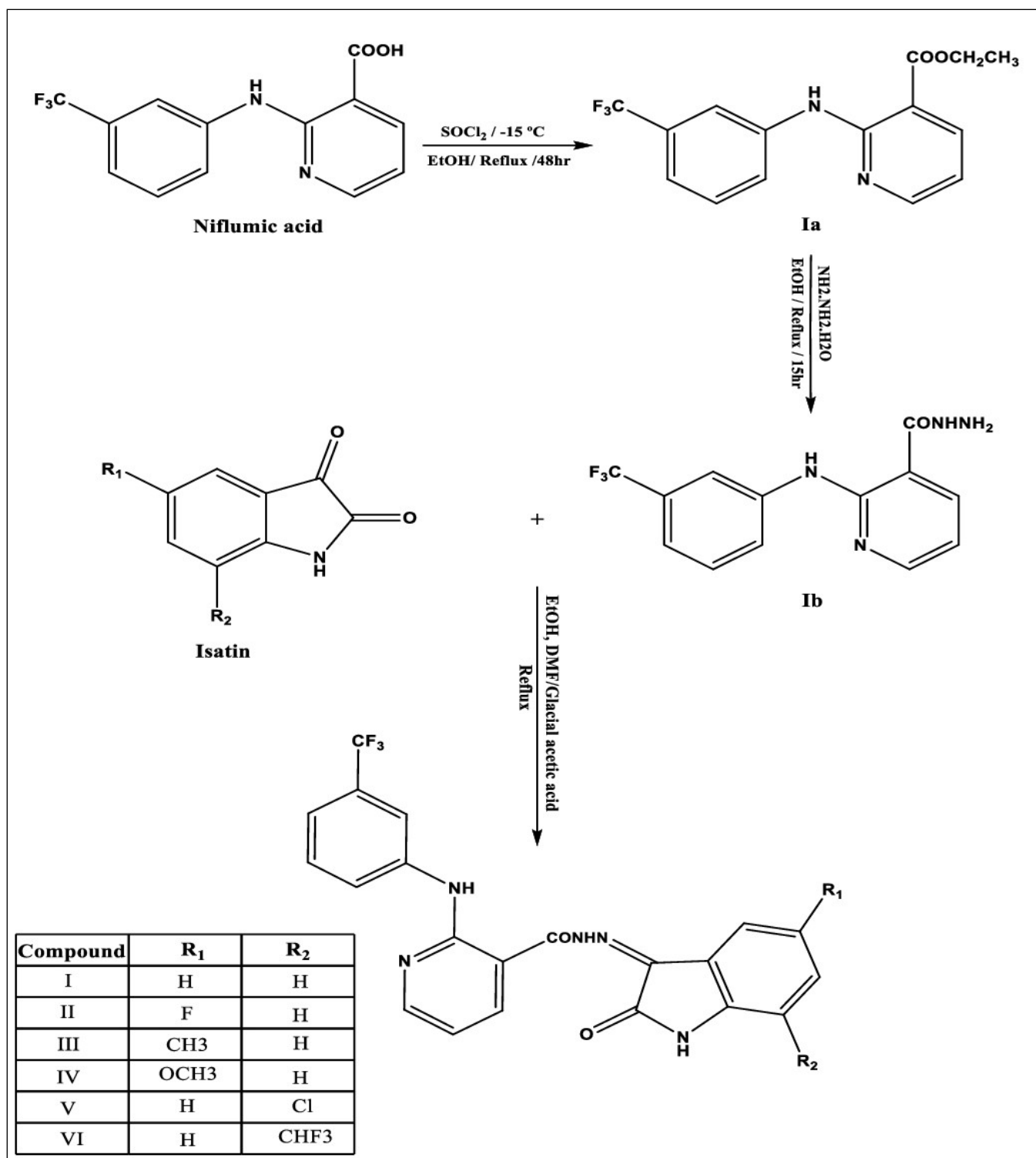


Fig. 1. Synthesis procedure of intermediates and final compounds

Source: Based on [19-20]

CHEMISTRY

SYNTHESIS OF NIFLUMIC ACID ETHYL ESTER (COMPOUND IA)

20 ml of dried ethanol was used to dissolve 2g (7.086 mmol) of Niflumic acid employing a 100 ml round-bottomed flask, the liquid was chilled to -15°C , and an

excess of thionyl chloride (1 ml, 13.78 mmol) was gradually added. The mixing process is initiated and the resulted mixture is allowed to gradually reach room temperature before refluxing at 78°C for 48 hours using a hot plate magnetic stirrer. Upon completion of the reaction, which was confirmed using the TLC identification technique, 3 g of sodium bicarbonate dissolved in

Table 1. Physical and chemical characteristics of the intermediates and final compounds

Compound	Empirical formula	Molecular weight (g/mol)	Appearance	Yield [%]	Melting point [°C]	Rf value
Ia	C ₁₅ H ₁₃ F ₃ N ₂ O ₂	310.28	Brown oil	65	-----	0.94
Ib	C ₁₃ H ₁₁ F ₃ N ₄ O	296.25	White to off-white crystals	80	144-145	0.36
I	C ₂₁ H ₁₄ F ₃ N ₅ O ₂	425.37	Yellow powder	72	295-297	0.60
II	C ₂₁ H ₁₃ F ₄ N ₅ O ₂	443.36	Brown powder	75	311-312	0.50
III	C ₂₂ H ₁₆ F ₃ N ₅ O ₂	439.40	Orange powder	65	310-311	0.63
IV	C ₂₂ H ₁₆ F ₃ N ₅ O ₃	455.40	Dark brown powder	60	289-291	0.56
V	C ₂₁ H ₁₃ ClF ₃ N ₅ O ₂	459.81	Brown powder	79	311-312	0.52
VI	C ₂₂ H ₁₃ F ₆ N ₅ O ₂	493.37	Light brown powder	77	263-264	0.45

Source: Based on [25]

30 ml of distillate water was incrementally introduced to the resultant mixture to neutralize the acidity resulting from HCl emission. The extraction technique is performed three times to ensure complete extraction of the oily ester layer using 30 ml ethyl acetate each time. The final organic layer is even more dried using an adequate amount of anhydrous sodium sulfate (Na₂SO₄) and then filtered [21-22].

SYNTHESIS OF NIFLUMIC ACID HYDRAZIDE (COMPOUND IB)

1.50 ml (8.89 mmol) of Niflumic acid ethyl ester (compound Ia) is dissolved in 15 ml of absolute ethanol. Subsequently, 0.6 ml (12.34 mmol) of 99% hydrazine hydrate is added gradually. The mixture is maintained at room temperature with gentle stirring for 3 hours before refluxing for 15 hours at 78°C using a hot plate magnetic stirrer. Following the confirmation of reaction completion via TLC observation, the solvent is evaporated under vacuum conditions, yielding a brown hydrazide powder. Recrystallization with a combination of ethanol and n-hexane is conducted to isolate the pure brown crystals of Niflumic acid hydrazide [23].

SYNTHESIS OF THE FINAL ACYL HYDRAZONE COMPOUNDS (COMPOUNDS I-VI)

Niflumic acid hydrazide 0.75g (2.53 mmol) was dissolved in a solvent combination of absolute ethanol and DMF in a 1:1 ratio. In a separate round-bottomed flask, the identical solvent combination was employed to individually dissolve 3.79 mmol of each Isatin derivative accompanied by a catalytic amount of glacial acetic acid (1-2 drops) [24]. Each Isatin derivative was combined separately with the hydrazide-containing solution. The resultant mixtures were subjected to reflux at 90°C for varying periods (20-48) hours (monitored by TLC technique) to produce the final acyl hydrazone com-

pounds. After that, the solution was evaporated under a reduced pressure technique, and the six resultant compounds were recrystallized using DCM and n-hexane, washed with diethyl ether, and allowed to dry. Table (1) shows the physical and chemical properties, along with the yield percent, of the obtained intermediates and compounds [25].

SPECTROSCOPIC EXAMINATION OF INTERMEDIATES AND FINAL COMPOUNDS

COMPOUND IA

FTIR (cm⁻¹): 3363 (N-H) strch of 2.nd amine, 2947, 2875 (CH) strch of aliph. (CH₂, CH₃), 1691 (C=O) strch. of conjugate ester, 1614 (C=N) strch, 1587, 1531, 1446 (aromatic C=C) strch, 1330 (C-F) strch, 1288 (C-O) strch, 1255 (C-N) strch.

COMPOUND IB

FTIR (cm⁻¹): 3415, 3309 (N-H) strch of 1.prim amine, 3041 (aromatic C-H) strch, 1608(C=O) strch of amide, 1587 (C=N) strch, 1525, 1462 (aromatic C=C) strch, (1336 C-F) strch 1255 (C-N) strch.

COMPOUND I

FTIR (cm⁻¹): 3236 (N-H) strch of 2.nd amine, 3041 (aromatic C-H) strch, 1695 (C=O) strch of amide, 1656 (C=N) strch of imine, 1622, 1591, 1463 (C=C) strch of aromatic, 1327 (C-F) strch, 1249 (C-N) strch.

¹H-NMR (400MHz, DMSO-d₆, ppm): 13.92 (singlet, 1H of amide N-H), 11.40 (singlet, 1H of N-H), 10.48 (singlet, 1H of indole N-H), 8.47-6.93 (multiplet, 11H of H-Ar).

COMPOUND II

FTIR (cm⁻¹): 3251 (N-H) strch of 2.nd amine, 3089 (aromatic C-H) strch, 1699 (C=O) strch of amide, 1653 (C=N)

Table 2. Docking outcomes of the reference drug and the synthesized compounds with the VEGF-R2 tyrosine kinase site (PDB code: 4AG8)

Compound	S. score (Kcal/mol)	RMSD	No. of binding sites	Binding amino acids
Sunitinib	-8.7276	2.0611	2	Asp 1046, Leu 840
I	-9.1782	1.5147	5	Asp 1046, Glu 885, Lys 868, Leu 889, Phe 1047
II	-9.2425	1.1745	4	Asp 1046, Glu 885, Lys 868, Leu 889
III	-9.4254	1.0608	4	Asp 1046, Glu 885, Phe 1047, Leu 889
IV	-9.2709	1.8914	4	Asp 1046, Glu 885, Lys 868, Leu 889
V	-9.2731	1.5234	4	Asp 1046, Glu 885, Lys 868, Leu 889
VI	-9.5120	1.3227	4	Asp 1046, Glu 885, Lys 868, Leu 889

Source: Own materials

strch vibration of imine, 1608, 1585, 1479 (C=C) strch, 1328 (C-F) strch, 1255 (C=N) strch.

¹H-NMR (400MHz, DMSO.d₆, ppm): 13.91 (singlet, 1H of amide N-H), 11.42 (singlet, 1H of N-H), 10.43 (singlet, 1H of indole N-H), 8.47-6.88 (multiplet, 10H of H-Ar).

COMPOUND III

FTIR (cm⁻¹): 3176 (N-H) strch of 2.nd amine, 3059 (aromatic C-H) strch, 2818 (aliph. CH₃) strch, 1695 (C=O) strch of amide, 1666 (C=N) strch of imine, 1593, 1533, 1444 (C=C) strch, 1327 (C-F) strch, 1251 (C-N) strch.

¹H-NMR (400MHz, DMSO.d₆, ppm): 13.93 (singlet, 1H of amide N-H), 11.31 (singlet, 1H of N-H), 10.48 (singlet, 1H of indole N-H), 8.48-6.82 (multiplet, 10H of H-Ar), 2.29 (singlet, 3H of CH₃).

COMPOUND IV

FTIR (cm⁻¹): 3170 (N-H) strch of 2.nd amine, 3055 (aromatic C-H) strch, 2835 (aliph. CH₃) strch, 1695 (C=O) strch of amide, 1666 (C=N) strch of imine, 1597, 1531, 1442 (C=C) strch, 1327 (C-F) strch, 1284 (C-O) strch, 1251 (C-N) strch.

¹H-NMR (400MHz, DMSO.d₆, ppm): 13.97 (singlet, 1H of amide N-H), 11.19 (singlet, 1H of N-H), 10.52

(Singlet, 1H of indole N-H), 8.48-6.81 (multiplet, 10H of H-Ar), 3.75 (singlet, 3H of CH₃).

COMPOUND V

FTIR (cm⁻¹): 3238 (N-H) strch of 2.nd amine, 3055 (aromatic C-H) strch, 1687 (C=O) strch of amide, 1664 (C=N) strch, 1612, 1583, 1446 (C=C) strch, 1332 (C-F) strch, 1249 (C-N) strch, 759 (C-Cl) strch.

¹H-NMR (400MHz, DMSO.d₆, ppm): 13.88 (singlet, 1H of amide N-H), 11.87 (singlet, 1H of N-H), 10.43 (singlet, 1H of indole N-H), 8.54-7.12 (multiplet, 10H of H-Ar).

COMPOUND VI

FTIR (cm⁻¹): 3205 (N-H) strch of 2.nd amine, 3082 (aromatic C-H) strch, 1701 (C=O) strch of amide, 1676 (C=N) strch, 1614, 1583, 1444 (C=C) strch, 1328 (C-F) strch, 1249 (C-N) strch.

¹H-NMR (400MHz, DMSO.d₆, ppm): 13.79 (singlet, 1H of amide N-H), 11.82 (singlet, 1H of N-H), 10.35 (singlet, 1H of indole N-H), 8.49-7.08 (multiplet, 10H of H-Ar).

DOCKING STUDY

The molecular docking program helps identify the ideal structural conformation and orientation using a specific algorithm, followed by a scoring function to predict binding affinity and assess the interaction mode. The primary protein structural database is the publicly accessible Protein Data Bank (PDB) [26]. The docking investigation comprises two primary parts. The first part deals with ligand preparation, which involves building the structure of the necessary derivatives using Chem Draw professional software version 12.0, followed by atoms protonation, charges, energy optimization, and structural energy minimization using the Molecular Operating Environment (MOE 2015) software [27-28]. The second part deals with target macromolecule or enzyme preparation, which requires importing the crystal structure of the VEGFR-2 kinase active site (PDB code: 4AG8) into the MOE software, subsequently removing water, ligand previously attached to the co-crystallized structure, active site protonation [29]. Following the preparation of the requisite active site, the receptor docking study commences to evaluate the binding energy values (S. score) and root mean square deviation (RMSD). Derivatives exhibiting an optimum S. score and a low RMSD will demonstrate optimal binding and compatibility with the target receptor site.

CYTOTOXIC STUDY

The National Cell Bank of Iran (Pasteur Institute, Iran) provided the human lung cancer cell line A549 and

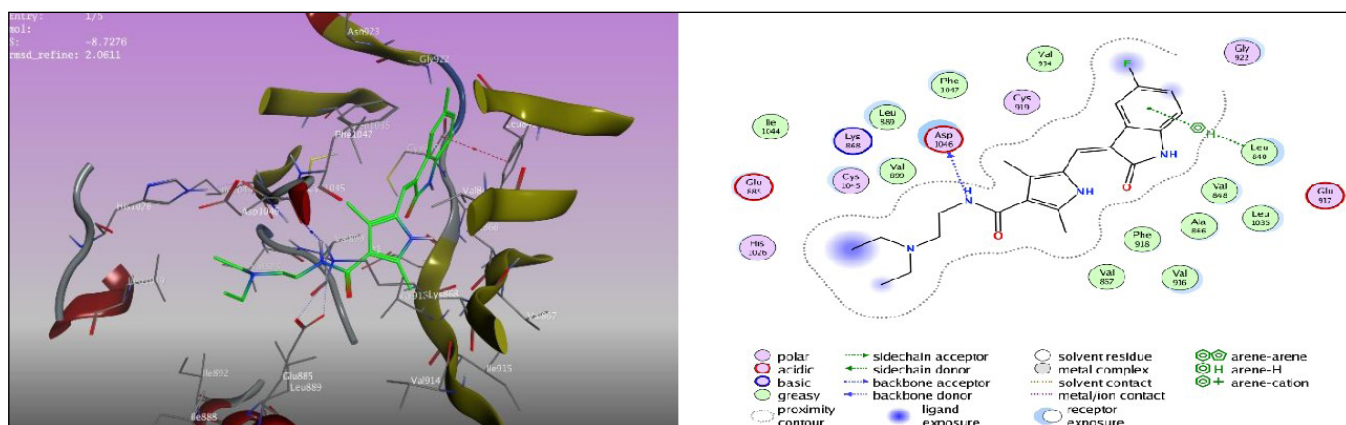


Fig. 2 Docking result of sunitinib with the VEGFR-2 tyrosine kinase (PDB code: 4AG8)

Source: Own materials

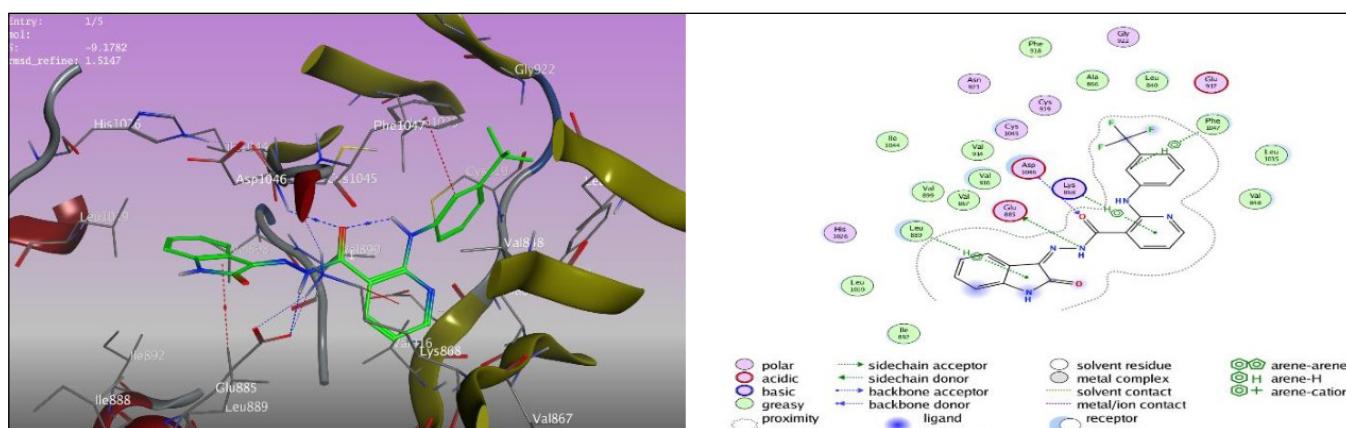


Fig. 3. Docking result of compound I with the VEGFR-2 tyrosine kinase (PDB code: 4AG8)

Source: Own materials

the normal lung fibroblast cell line MRC-5. Cells had been grow in RPMI-1640 media (Gibco) with 10% fetal bovine serum (FBS) and antibiotics, such as 100 U/mL penicillin and 100 µg/mL streptomycin. Cells were kept alive in a humidified incubator at 37 °C with 5% CO₂. We used a trypsin-EDTA solution to separate the cells and then rinsed them with phosphate-buffered saline (PBS)) [30].

MTT VIABILITY ASSAY

The MTT assay was carried out to assess the capacity for survival of the cells. A density of 1.4×10^4 cells/well was used to seed cells in 96-well plates, and the cells were incubated for 24 hours. MTT solution (0.5 mg/mL) was introduced and incubated for 4 hours after the test compounds were treated with a range of concentrations (6.25–100 µg/mL) for an additional 24 hours. The formazan crystals that were produced were dissolved in DMSO, and the absorbance was measured at 570 nm using a microplate reader. The dose-response data was used to calculate the IC₅₀ values [31].

RESULTS

CHEMISTRY

The esterification of Niflumic acid was accomplished using ethanol as solvent, with thionyl chloride added under chilled conditions to generate the acid chloride, which rapidly interacts with ethanol to produce the ethyl ester of Niflumic acid, which was observed by the disappearance of broad OH peak of carboxylic acid and appearance of C=O group of conjugate esters at 1691 cm⁻¹. The synthesized ester was subsequently reacted with hydrazine monohydrate 99% to produce the hydrazide. The carbonyl of the ester vanished, whereas the amide C=O band appeared at 1608 cm⁻¹, with the primary amine group at 3415, 3309 cm⁻¹. The obtained hydrazide compound then reacted with ketone containing compound to form the final acyl hydrazone compounds, which is observed utilizing FTIR and HNMR by replacement of primary amine group bands with secondary amine single band near 3200 cm⁻¹ and the appearance of sharp imine group band at the range 1653-1676 cm⁻¹ while the ¹HNMR showed three singlet hydrogen peaks of secondary amine containing compounds above 10.40 ppm.

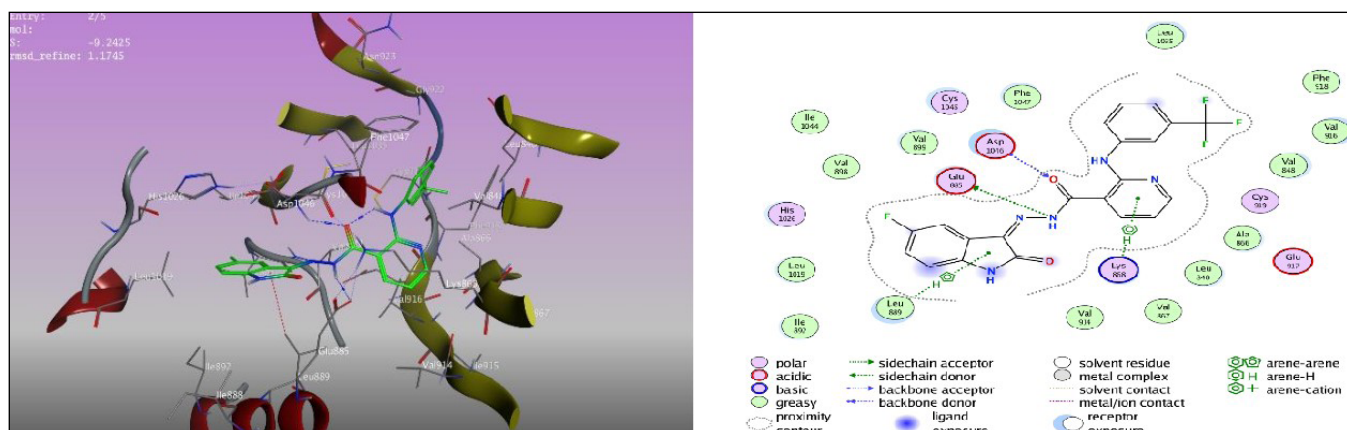


Fig. 4. Docking result of compound II with the VEGFR-2 tyrosine kinase (PDB code: 4AG8)

Source: Own materials

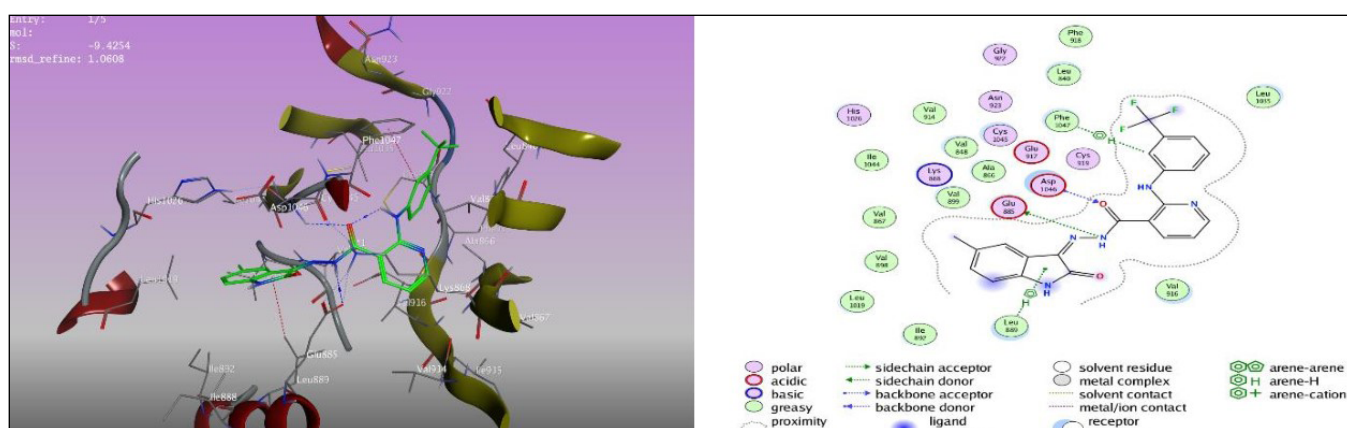


Fig. 5: Docking result of compound III with the VEGFR-2 tyrosine kinase (PDB code: 4AG8)

Source: Own materials

DOCKING STUDY

The docking results show enhanced binding energy (S. score) equal -9.1782 to -9.5120 Kcal/mol and optimum binding mode (RMSD) values equal 1.0608 to 1.8914 with the target VEGFR-2 kinase domain (PDB code: 4AG8) as a compared with the reference drug (Sunitinib) which shows S. score value equal -8.7276 Kcal/mol and RMSD value equal 2.0611. The synthesized six compounds show an additional four to five interactions with crucial amino acids involved in the gatekeeper region (Lys 868), the catalytic DFG motif (Glu885, Asp1046) and the allosteric hydrophobic pocket. As illustrated in Figures 2–8, these interactions demonstrate the strong binding affinity and stability of the synthesized ligands within the VEGFR-2 active site. Table (2) displays the docking outcomes of the final compounds with their first to second poses with the target VEGFR-2 tyrosine kinase active compared with the reference ligand (Sunitinib) interactions at the same site.

CYTOTOXIC STUDY

In this study, six novel compounds were synthesized, and their cytotoxic effects were evaluated using adenocarci-

nomic human alveolar basal epithelial cell (A549) and a normal diploid fibroblast from human fetal lung tissue (MRC-5). The MTT cell viability assay was employed to assess the effect of the synthesized compounds and the reference drug (Sunitinib) on the two cell lines; each IC₅₀ value was determined using different concentrations of reference and synthesized compounds. The IC₅₀ values represent the compound concentration at which 50% of cells become non-viable. The results demonstrated very promising cytotoxic results for the synthesized compounds and a safer effect on normal cells as compared with the reference drug (Sunitinib). The IC₅₀ levels of the produced compounds against the cell lines varied from 20.87 μM to 78.48 μM in the A549 cell line and from 175.49 μM to 280.27 μM in the MRC-5 cell line. The most pronounced inhibitory effect was noted with compound II. Both Figures (9-10) displays the relationship between concentration and impact by plotting the viability data of A549 and MRC-5 cells against the respective concentrations of the reference and synthesized compounds. The Statistical Analysis System (SAS) application version 2018 was utilized to identify the impact of various vari-

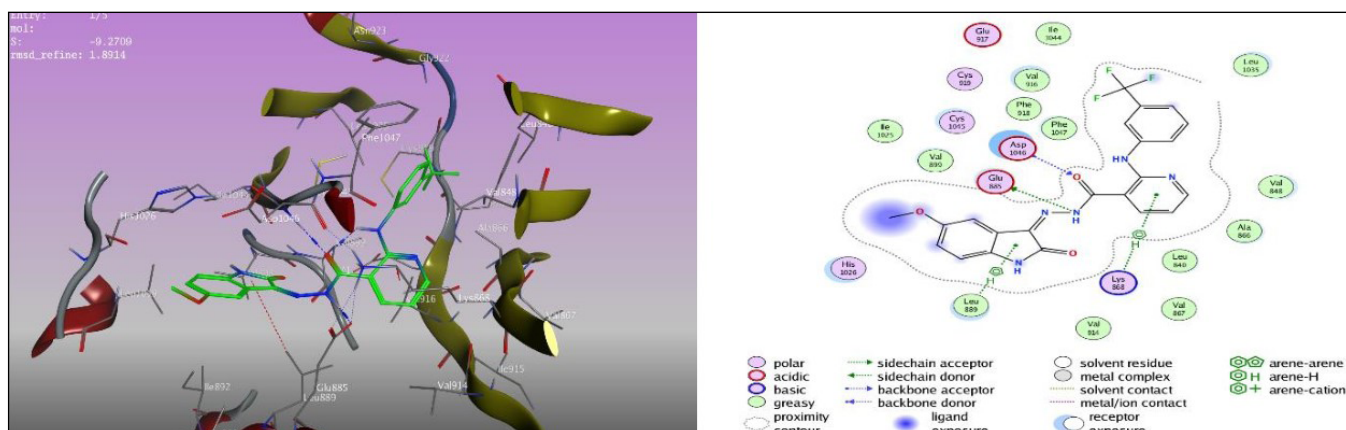


Fig. 6. Docking result of compound IV with the VEGFR-2 tyrosine kinase (PDB code: 4AG8)

Source: Own materials

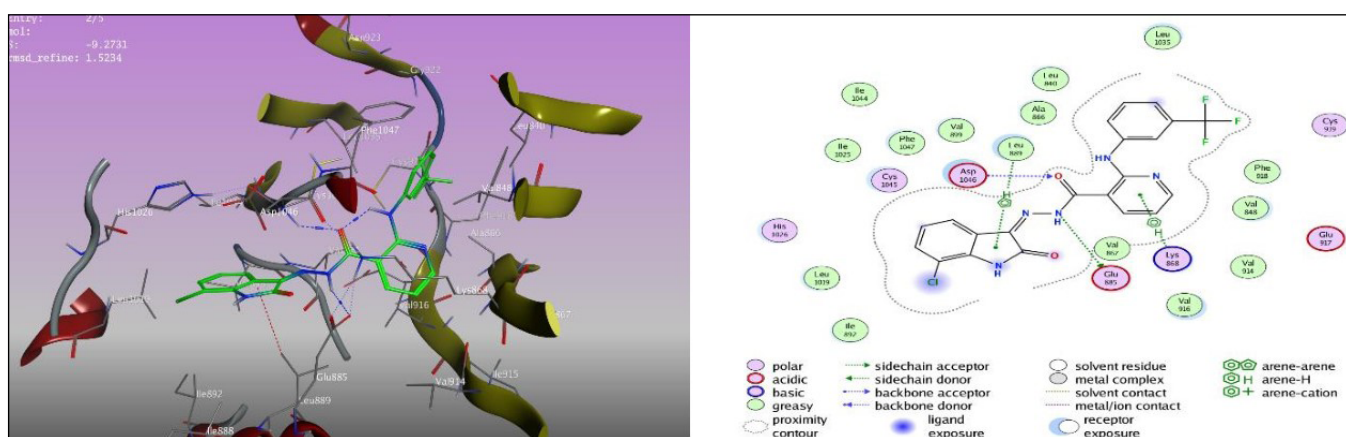


Fig. 7. Docking result of compound V with the VEGFR-2 tyrosine kinase (PDB code: 4AG8)

Source: Own materials

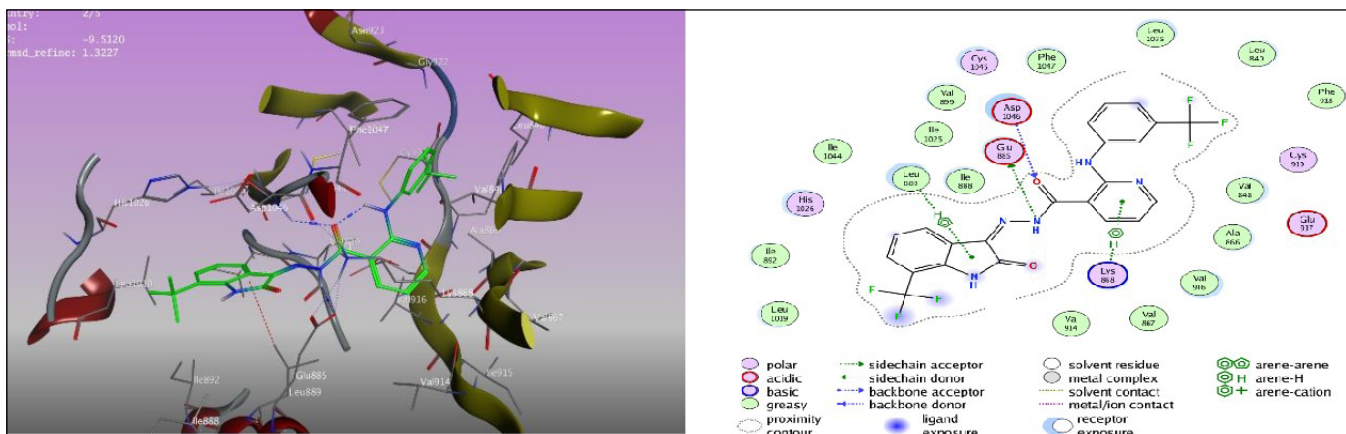


Fig. 8. Docking result of compound VI with the VEGFR-2 tyrosine kinase (PDB code: 4AG8)

Source: Own materials

ables on research parameters. The T-test was employed to significantly compare the means in this investigation as shown in table (3).

DISCUSSION

The docking results indicate that the synthesized compounds have stronger binding affinities and

more stable binding conformations than the reference drug Sunitinib, as reflected by their more negative S. score values and smaller RMSD values. The observed interactions with crucial amino acids in the VEGFR-2 kinase active site, such as those in the gatekeeper region, the DFG motif, and the allosteric site, suggest that the designed compounds provide enhanced inhibition of VEGFR-2 kinase activity. The

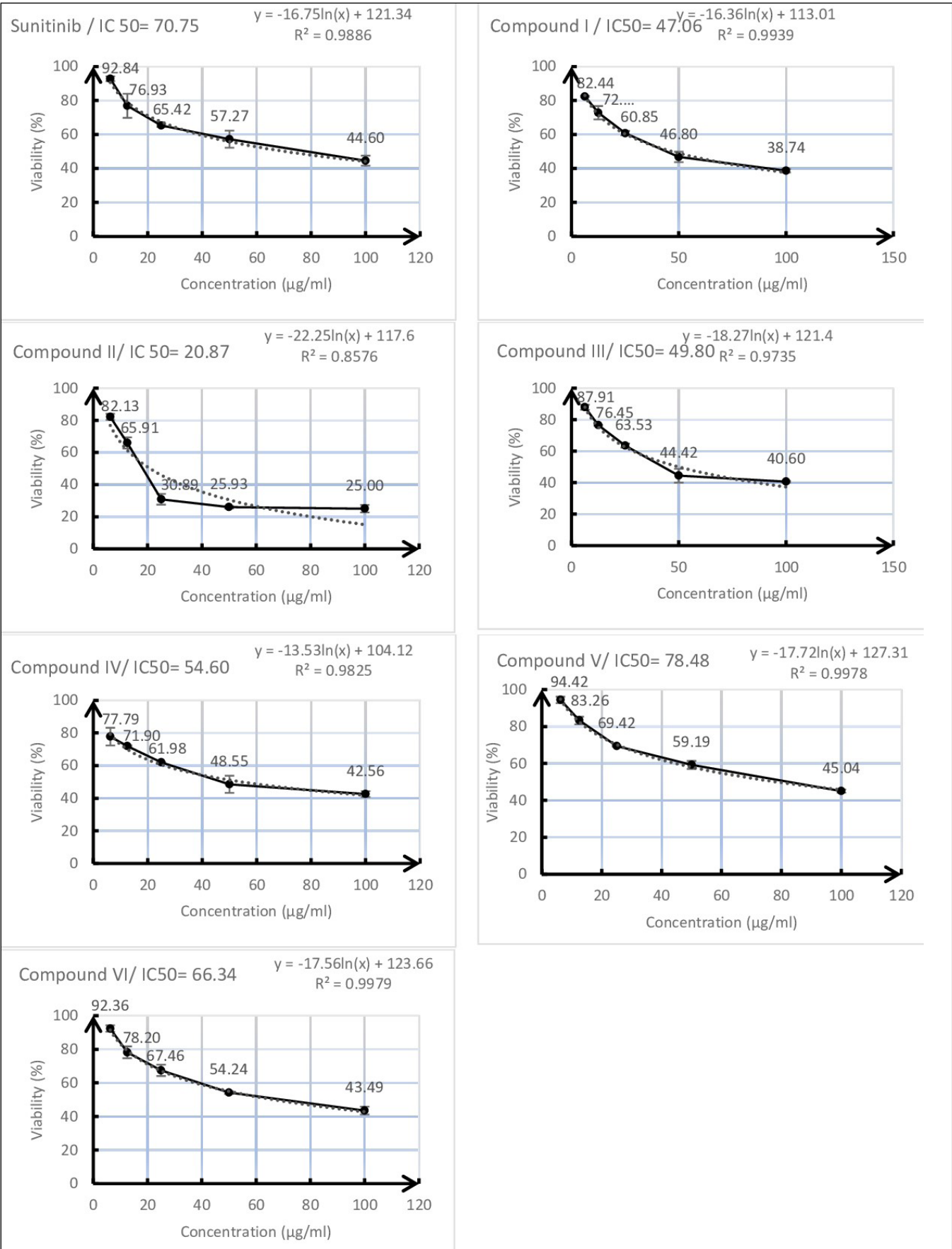
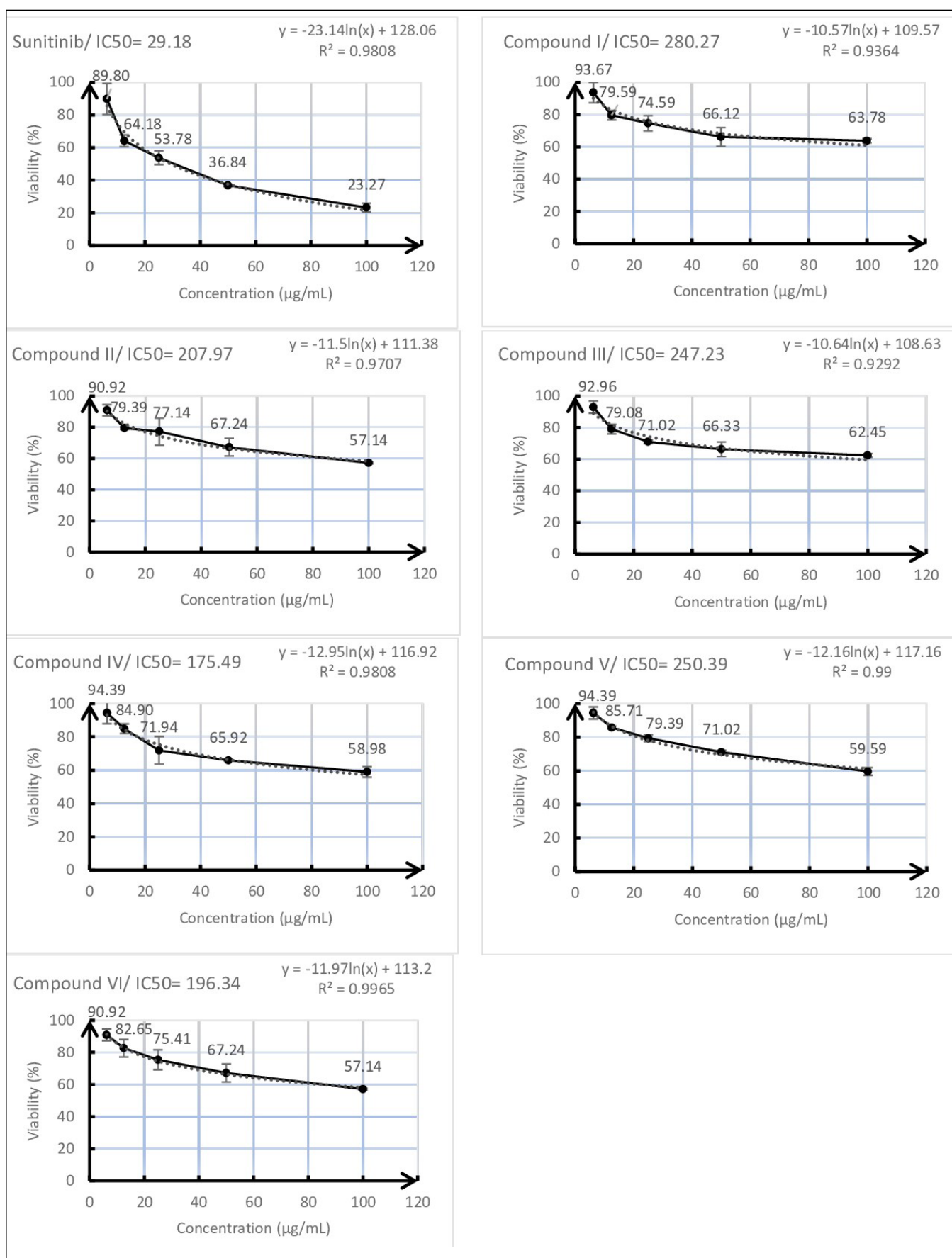


Fig. 9. Cytotoxicity result of the standard and synthesized compound on A549 cell line
Source: Own materials

**Fig. 10.** Cytotoxicity result of the standard and synthesized compound on MRC-5 cell line

Source: Own materials

Table 3. IC50 values for the tested compounds and standard. The values are represented by the mean ± SD of triplicate measurements in A549 and MRC-5

Compound	A549		MRC-5	
	IC50 ±SD	P-value	IC50 ±SD	P-value
Sunitinib	70.75 ±2.81	Standard	29.18 ±1.55	Standard
I	47.06 ±2.07	0.0004 ** a	280.27 ±26.03	0.0001 ** a
II	20.87 ±1.29	0.0001 ** a	207.97 ±17.94	0.0001 ** a
III	49.80 ±3.16	0.0005 ** a	247.23 ±22.41	0.0001 ** a
IV	54.60 ±2.78	0.0017 ** a	175.49 ±9.76	0.0001 ** a
V	78.48 ±4.52	0.0381 * a	250.39 ±13.60	0.0001 ** a
VI	66.34 ±3.70	0.237 NS	196.34 ±9.96	0.0001 ** a

Notes: a - Significant difference that the comparison with Sunitinib, NS - Non-significant; * (P<0.05), ** (P<0.01), NS: Non-significant
Source: Own materials

presence of additional interactions compared to Sunitinib implies improved specificity and potential biological activity. The synthetic pathway demonstrates a successful stepwise conversion from Niflumic acid to its ester, then to hydrazide, and finally to the acyl hydrazone derivatives. The use of thionyl chloride effectively activated the carboxylic acid group, facilitating ester formation. The disappearance of the hydroxyl group and the appearance of the aliphatic ethyl carbones in FTIR confirmed the esterification. The subsequent formation of hydrazide was evident from the frequency downshifting of the amide carbonyl and appearance of 2.nd amine bands. Finally, the formation of the acyl hydrazones was supported by both FTIR and ¹HNMR data, particularly the imine band and the downfield-shifted singlet peaks in the ¹HNMR spectrum. These spectral changes confirm the success of each reaction step and the formation of the final compounds along with their intermediates. The cytotoxic data suggest that the synthesized compounds exhibit promising tumor-selective cytotoxicity, showing enhanced inhibition of cancer cell viability while maintaining reduced toxicity toward normal cells compared to the reference drug and previously reported studies. This selective effect may

be attributed to the overexpression of VEGFR-2 in the A549 cancer cells, increasing compound uptake or binding. Compound II high activity is likely due to its strong electron-withdrawing substituents, which reduce electron density, and the low steric hindrance of the fluorine atom, enabling more efficient interaction with the kinase binding site. These structural features may contribute to improved binding affinity and inhibitory efficacy, supporting its potential as a lead compound for further development.

CONCLUSIONS

A set of isatin-niflumic acid derivatives (I-VI) have been successfully synthesized, and their chemical structures were confirmed using FTIR and ¹HNMR methods. The molecular docking studies and MTT assays for the assessed drugs revealed a robust correlation between the predicted results from molecular docking and the biological evaluations, demonstrating notable selectivity towards the VEGFR-2 kinase active site. In summary, the newly synthesized niflumic acid derivatives serve as potent anticancer medicines by blocking VEGFR tyrosine kinase, hence restricting cell development and possesses promise as targets for additional studies on anticancer treatments.

REFERENCES

1. Housman G, Byler S, Heerboth S, Lapinska K, Longacre M, Snyder N, et al. Drug resistance in cancer: An overview. *Cancers* (Basel). 2014 Sep 5;6(3):1769–1792. doi: 10.3390/cancers6031769. DOI

2. De Las Rivas J, Brozovic A, Izraely S, Casas-Pais A, Witz IP, Figueroa A. Cancer drug resistance induced by EMT: novel therapeutic strategies. *Arch Toxicol*. 2021 Jul; 95(7):2279-2297. doi: 10.1007/s00204-021-03063-7.

3. Anand U, Dey A, Chandel AKS, Sanyal R, Mishra A, Pandey DK, et al. Cancer chemotherapy and beyond: Current status, drug candidates, associated risks and progress in targeted therapeutics. *Genes Dis*. 2022 Mar 18;10(4): 1367-1401. doi: 10.1016/j.gendis.2022.02.007. DOI

4. Ghalehbandi S, Yuzugulen J, Pranjol MZI, Pourgholami MH. The role of VEGF in cancer-induced angiogenesis and research progress of drugs targeting VEGF. *Eur J Pharmacol*. 2023 Jun 15;949:175586. doi: 10.1016/j.ejphar.2023.175586.

5. Li F, Xu J, Liu S. Cancer stem cells and neovascularization. *Cells* 2021;10(5):1070. Doi: 10.3390/cells10051070

6. Riquelme E, Suraokar M, Behrens C, Lin HY, Girard L, Nilsson MB, et al. VEGF/VEGFR-2 upregulates EZH2 expression in lung adenocarcinoma cells and EZH2 depletion enhances the response to platinum-based and VEGFR-2-targeted therapy. *Clin Cancer Res*. 2014 Jul 15; 20(14): 3849-61. doi: 10.1158/1078-0432.CCR-13-1916.
7. Liu XJ, Zhao HC, Hou SJ, Zhang HJ, Cheng L, Yuan S, et al. Recent development of multi-target VEGFR-2 inhibitors for the cancer therapy. *Bioorg Chem*. 2023 Apr;133:106425. doi: 10.1016/j.bioorg.2023.106425.
8. Shah FH, Nam YS, Bang JY. et al. Targeting vascular endothelial growth receptor-2 (VEGFR-2): structural biology, functional insights, and therapeutic resistance. *Arch Pharm. Res*. 2025;48:404-425. doi: 10.1007/s12272-025-01545-1. DOI
9. Elkaeed EB, Yousef RG, Khalifa MM, et al. Discovery of New VEGFR-2 Inhibitors: Design, Synthesis, Anti-Proliferative Evaluation, Docking, and MD Simulation Studies. *Molecules*. 2022 Sep 21;27(19):6203. doi: 10.3390/molecules27196203.
10. Samadani AA, Keymoradzdeh A, Shams S, et al. Mechanisms of cancer stem cell therapy. *Clin Chim Acta*. 2020 Nov;510:581-592. doi: 10.1016/j.cca.2020.08.016.
11. Abdelsalam EA, Abd El-Hafeez AA, Eldehna WM, et al. Discovery of novel thiazolyl-pyrazolines as dual EGFR and VEGFR-2 inhibitors endowed with in vitro antitumor activity towards non-small lung cancer. *J Enzyme Inhib Med Chem*. 2022 Dec;37(1): 2265-2282. doi: 10.1080/14756366.2022.2104841.
12. Modi SJ, Kulkarni VM. Vascular Endothelial Growth Factor Receptor (VEGFR-2)/KDR Inhibitors: Medicinal Chemistry Perspective. *J Comput Aided Mol Des*. 2015 Aug; 29(8):757-76. doi: 10.1007/s10822-015-9859-y.
13. Alibeg A, Mohammed M. Design, synthesis, insilco study and biological evaluation of new Isatin-sulfonamide derivatives by using mono amide linker as possible as histone deacetylase inhibitors. *Pol Merkur Lekarski*. 2024;52(2):178-188. doi: 10.36740/Merkur202402106.
14. Cheke RS, Patil VM, Firke SD, et al. Therapeutic Outcomes of Isatin and Its Derivatives against Multiple Diseases: Recent Developments in Drug Discovery. *Pharmaceuticals*, 2022;15(3), 272. doi: 10.3390/ph15030272 DOI
15. Luo S, Huang G, Wang Z, et al. Niflumic acid exhibits anti-tumor activity in nasopharyngeal carcinoma cells through affecting the expression of ERK1/2 and the activity of MMP2 and MMP9. *Int J Clin Exp Pathol*. 2015 Sep 1;8(9):9990-10001.
16. Gómez-Betancur I, Zhao J, Tan L, et al. Bioactive Compounds Isolated from Marine Bacterium *Vibrio neocaledonicus* and Their Enzyme Inhibitory Activities. *Mar Drugs*. 2019 Jul 8;17(7):401. doi: 10.3390/md17070401. DOI
17. Kowalska T, Sajewicz M. Thin-Layer Chromatography (TLC) in the Screening of Botanicals—Its Versatile Potential and Selected Applications. *Molecules* 2022;27(19):6607. Doi: 10.3390/molecules27196607.
18. Nazarski RB. On the Use of Deuterated Organic Solvents without TMS to Report ¹H/¹³C NMR Spectral Data of Organic Compounds: Current State of the Method, Its Pitfalls and Benefits, and Related Issues. *Molecules*. 2023 May 26;28(11):4369. doi: 10.3390/molecules28114369.
19. Agbese SA, Shallangwa GA, Idris SO. Synthesis, characterization and antimicrobial evaluation of co(II), ni(II) and cu(II) schiff base complexes of (Z)-4-(1-pyridin-4-ylimino) propyl)phenol. *Trop J Nat Prod Res*. 2018 Sep 1;2(9):429-32. doi.org/10.26538/tjnpr/v2i9.4.
20. Narajji C, Karvekar MD, Das AK. Biological Importance of Organoselenium Compounds. *Indian J Pharm Sci*. 2007;69 (3):344-351. doi: 10.4103/0250-474X.34541 DOI
21. Li J, Sha Y. A convenient synthesis of amino acid methyl esters. *Molecules* 2008;13(5):1111-1119. doi: 10.3390/molecules13051111. DOI
22. Fihurka N, Tarnavchik I, Samaryk V, et al. A Study of an Irreversible Condensation of Glutamic Acid and Polyoxyethylene/Polyoxypropylene Diols Using Thionyl Chloride. *Org Prep Proced Int*. 2018 Sep 3;50(5):502-8. doi: 10.1080/00914037.2023.2274591. DOI
23. Boulebd H, Zine Y, Khodja IA, Mermer A, Demir A, Debache A. Synthesis and radical scavenging activity of new phenolic hydrazone/hydrazide derivatives: Experimental and theoretical studies. *J Mol Struct*. 2022;1249:131546. doi: 10.1016/j.molstruc.2021.131546. DOI
24. Mali SN, Thorat BR, Gupta DR, Pandey A. Mini-Review of the Importance of Hydrazides and Their Derivatives - Synthesis and Biological Activity. *Eng Proc*. 2021;11(1):21. doi: 10.3390/ASEC2021-11157. DOI
25. Uddin N, Rashid F, Ali S, et al. Synthesis, characterization, and anticancer activity of Schiff bases. *J Biomol Struct Dyn*. 2020 Jul; 38(11): 3246-3259. doi: 10.1080/07391102.2019.1654924.
26. Burley SK, Berman HM, Duarte JM, et al. Protein Data Bank: A Comprehensive Review of 3D Structure Holdings and Worldwide Utilization by Researchers, Educators, and Students. *Biomolecules*. 2022 Oct 4; 12(10):1425. doi: 10.3390/biom12101425.
27. Trott O, Olson AJ. Auto Dock Vina: Improving the speed and accuracy of docking with a new scoring function, efficient optimization, and multithreading. *J Comput Chem*. 2010 Jan 30;31(2): 455-61. doi: 10.1002/jcc.21334.
28. Alsayad HH, Aziz Alibeg AA, Rad Oleiwi ZK. Molecular Docking, Synthesis, Characterization, and Preliminary Cytotoxic Study of Novel 1, 2, 3-Triazole-Linked Metronidazole Derivatives. *Adv J Chem Sect A*. 2024 Nov 1;7(6):797-809. doi: 10.48309/AJCA.2024.464130.1570. DOI
29. Yang C, Chen EA, Zhang Y. Protein-Ligand Docking in the Machine-Learning Era. *Molecules*. 2022 Jul 18;27(14):4568. doi: 10.3390/molecules27144568.
30. Xu XY, Nie XC, Ma HY, et al. Flow Cytometry Method Analysis of Apoptosis: No Significant Difference Between EDTA and EDTA-free Trypsin Treatment Procedure. *Technol Cancer Res Treat*. 2015 Apr;14(2):237-41. doi: 10.7785/tcrt.2012.500406.

31. Luzak B, Siarkiewicz P, Boncler M. An evaluation of a new high-sensitivity Presto Blue assay for measuring cell viability and drug cytotoxicity using EA.hy926 endothelial cells. *Toxicol In Vitro*. 2022 Sep;83:05407. doi: 10.1016/j.tiv.2022.105407.

CONFLICT OF INTEREST

The Authors declare no conflict of interest

CORRESPONDING AUTHOR

Hussein Muneam Sahib

Department of Pharmaceutical Chemistry

Faculty of Pharmacy, University of Kufa,

Najaf, Iraq

e-mail: husseinm.shmrtoa@student.uokufa.edu.iq

ORCID AND CONTRIBUTIONSHIP

Hussein Muneam Sahib: 0009-0003-3740-5597 **B** **C** **D** **E**

Ammar AbdulAziz Alibeg: 0000-0002-0974-1433 **A** **F**

A – Work concept and design, **B** – Data collection and analysis, **C** – Responsibility for statistical analysis, **D** – Writing the article, **E** – Critical review, **F** – Final approval of the article

RECEIVED: 21.06.2025

ACCEPTED: 13.10.2025

